Characterization of the Reaction Center Bound Tetraheme Cytochrome of *Rhodocyclus tenuis*

Laure Menin,[‡] Barbara Schoepp,[§] Daniel Garcia,[‡] Pierre Parot,[‡] and André Verméglio*[,‡]

C. E. A., DEVM-LBC, C. E. A. Cadarache, 13108 Saint-Paul-lez-Durance Cedex, France, and Laboratoire d' Ingénierie des Protéines, Centre de Génétique Moléculaire, CNRS, 91198 Gif-sur-Yvette Cedex, France

Received May 16, 1997; Revised Manuscript Received July 23, 1997[⊗]

ABSTRACT: Properties of the tetrahemic reaction center bound cytochrome have been investigated by different techniques. The mid-point potentials of the four hemes were determined by redox titration. The best fit of the data was obtained with a ($n = 1$) Nernst curve by using the following values of the redox parameters: $E_m = +420$ mV for the two high-potential hemes and $E_m = +110$ and $+60$ mV for the two low-potential hemes. The mid-point potentials of the two high-potential hemes are the highest reported so far. The spectral properties of the four hemes in the α-band have been determined by absorption spectroscopy and measurements of light-induced difference spectra in membranes of *Rhodocyclus tenuis.* The two high potential hemes present very similar spectra centered at 557 nm. The absorption spectra of the two low-potential hemes are very similar, and their α-band centered around 551 nm. Spectral properties at 100 K and the linear dichroism of optical transitions allow the determination of the relative orientations of the hemes with respect to the membrane plane. The orientation patterns thus obtained corresponds to none of the arrangements described so far for reaction center bound cytochromes.

In anoxygenic photosynthetic eubacteria, the photo-oxidized primary electron donor (P^+) is rapidly rereduced by a secondary electron donor (in the time range between 100 ns and several hundreds of microseconds depending upon the species). This fast rereduction prevents wasteful back electron transfer from the semiquinone states of the primary and secondary acceptors. For some species, such as *Rhodobacter (Rb.)*[1] *sphaeroides*, the secondary electron donor is a soluble cyt c_2. However, the great majority of the bacteria of the proteobacterial phylum uses a RC bound cytochrome as immediate reductant for the photo-oxidized primary donor P^+. Examples for such situations are also found in other phyla of the anoxygenic photosynthetic bacteria, i.e., green filamentous (Bruce et al., 1982), green sulfur (Prince & Olson, 1976), and heliobacteria (Prince et al., 1985). The degree of association of this subunit to the RC varies significantly between species. In *Rhodopseudomonas (Rp.) viridis*, this subunit is retained even in highly purified RC samples (Clayton & Clayton, 1978) whereas in *Rubrivivax (Ru.) gelatinosus* (Prince et al., 1978), it is easily released into the aqueous phase during purification. This RC bound cytochrome contains two high-potential (HP) and two low-potential hemes (LP). These four hemes have been characterized for many different species, *Rp. viridis* (Dracheva et al., 1988), *Chromatium (C.) vinosum* (Dutton, 1971; Case & Parson, 1971, 1973; Alegria & Dutton, 1990; Nitschke et al., 1993), *Ru. gelatinosus* (Dutton, 1971; Matsuura et al., 1988; Nitschke et al., 1992), *Rhodoferax (Rf.) fermentans* (Hochkoeppler et al., 1993, 1995), *Roseobacter (R.) denitrificans* (Garcia et al., 1994), and *Chloroflexus aurantiacus* (Zannoni & Venturoli, 1988; Freeman & Blankenship, 1990; Van Vliet et al., 1991), in terms of redox mid-point potentials (E_m), α-band absorption wavelengths, and orientation of the heme planes with respect to the membrane. A detailed picture, however, has only been available after the structural resolution of the *Rp. viridis* reaction center by X-ray crystallography. This structure has revealed the presence of four individual nonequivalent hemes arranged almost linearly (Deisenhofer et al., 1985) spanning a large part of the periplasmic space. The row of hemes is inclined by about 30° with respect to the membrane normal. Several different approaches [measurements of linear dichroism (LD) and EPR spectra in oriented samples, electron transfer kinetics between the hemes] have lead to the following alignment: P/*c*-559, (+380 mV)/*c*-552, (+20 mV)/*c*-556, (+320 mV)/*c*-554, (−60 mV) (Dracheva et al., 1988; Fritzsch et al., 1989; Nitschke & Rutherford, 1989; Verméglio et al., 1989a,b; Alegria & Dutton, 1991). Subsequent studies have shown that the overall organization of the *Rp. viridis* tetraheme subunit is compatible with data obtained from *Ru. gelatinosus* (Nitschke et al., 1992), *C. vinosum* (Nitschke et al., 1993), and *R. denitrificans* (Garcia et al., 1994). However, in contrast to the highly conserved orientation of the cofactors in the RC core proteins (Deisenhofer et al., 1985; Allen et al., 1986), the organization and the redox potentials of the tetraheme are variable. For example, the orientation and E_m values, determined in *Ru. gelatinosus* and *C. vinosum* by EPR (Nitschke et al., 1992, 1993) and in *R. denitrificans* by LD (Garcia et al., 1994), are different from those seen in the *Rp. viridis* cyt subunit. The nonconservation of heme orientations between species

* Corresponding author. Phone: 33 442254630. Fax: 33 442254701. E-mail: Vermeglio@DRA.CAD.CEA.FR.

‡ CEA Cadarache.

§ Centre de Génétique Moléculaire.

⊗ Abstract published in *Advance ACS Abstracts,* September 15, 1997.

[1] Abbreviations: Bpheo, bacteriopheophytin; cyt, cytochrome; E_h, ambient redox potential; E_m, midpoint potential; EPR, electron paramagnetic resonance; HiPIP, high-potential iron-sulfur protein; HP, high potential; LP, low potential; LD, linear dichroism; RC, reaction center; *C., Chromatium*; *R., Roseobacter*; *Rb., Rhodobacter*; *Rp., Rhodopseudomonas*; *Rc., Rhodocyclus; Rf., Rhodoferax; Ru., Rubrivivax*.

S0006-2960(97)01162-8 CCC: $14.00 © 1997 American Chemical Society

is consistent with the low sequence homology in the regions of the tetraheme cyt in contact with the RC (Nitschke et al., 1993). The data cited above and a comparison between the available amino acid sequences of various tetraheme cyt subunits strongly suggest that these proteins present a global common structure, but the orientation and electrochemical characteristics are fine tuned depending upon the species (Nitschke & Dracheva, 1995). The organization of the tetraheme cyt raises the following questions: (1) why are the four hemes arranged in an alternating sequence of redox potentials, (2) is this alternating sequence a common feature of all the tetraheme cyt, (3) what is the respective function of the four hemes, and (4) what is the sequence of electron flow through all four hemes toward P^+. The consensus on the role of the HP hemes is that their photo-oxidation is followed by their rereduction by a soluble electron carrier to complete the light-induced cyclic electron transfer (Meyer & Donohue, 1995). Although LP hemes can rapidly rereduce the photo-oxidized primary donor P^+, no clear role has been yet assigned to these two hemes. Schoepp et al. (1995) have shown that under anaerobic conditions, the LP hemes of *Ru. gelatinosus* are photo-oxidized by an actinic flash but they do not seem to be involved in an efficient cyclic electron transfer. A tentative explanation is that the LP hemes might serve as entry points for electrons coming from low-potential substrates (Dutton & Prince, 1978). Alternatively, the LP hemes may be necessary for an appropriate folding and structure of the tetraheme subunit.

The study of the tetraheme cyt organization in different species should provide a basis for better understanding the above questions. *Rhodocyclus (Rc.) tenuis* belongs to the β-subdivision of bacteria and appears to be closely related to *Ru. gelatinosus*. Recently, Agalidis et al. (1997) purified and characterized the RC of *Rc. tenuis*, but the tetraheme cyt *c* was lost during purification. *Rc. tenuis* offers a particular interest because it contains two high redox potential soluble electron donors in the periplasmic space, a HiPIP, and a cyt c_8, which are putative electron donors to the HP hemes to complete the light-induced cyclic electron transfer. In the present work, we have characterized the RC bound cytochrome of *Rc. tenuis* in terms of redox mid-point potentials, α-band wavelength positions, and relative orientations of the four hemes.

MATERIALS AND METHODS

Cells Growth. Cells of *Rc. tenuis* were grown in Hutner medium at 30 °C in anaerobic conditions under continuous illumination. The LHII peripheral antenna complex of *Rc. tenuis* contains a carotenoid belonging to the spirilloxanthin series with absorption maxima at 465, 492−495, and 528 nm (Hu et al., 1996). Large absorption changes in the carotenoid spectral region are observed under flash excitation due to the carotenoid electrochromic response (not shown). These changes overlap in the α-band region with those of cytochromes. Therefore, blue-green cells of *Rc. tenuis* have been obtained by addition of diphenylamine, a specific inhibitor of the carotenoids synthesis (Malhotra et al., 1969; Davies & Than, 1974), to the growth medium (final concentration = 10 μg/mL).

Preparation of Membranes and LHI−RC Complexes. Membranes were prepared as described by Schoepp et al. (1995). Particles of the photoreceptor complex (LHI−RC) were prepared according to Hu et al. (1996). The membranes (A_{870} = 50) were suspended in 10 mM Tris-HCl, 2 M NaBr, 0.2 M sucrose, and 50 mM glycyl/glycine (30 min in ice), diluted 1:1 in 50 mM glycyl/glycine and ultracentrifuged at 255000*g* for 90 min. The pellet, resuspended in 50 mM potassium phosphate buffer (pH 8) (A_{870} = 50), was treated for 60 min in an ice bath by a mixture of detergents Deriphat-160 (Henkel) and *n*-octyl-β-D-glucoside (Sigma) at a final concentration of 3 and 1%, respectively. The solution was then diluted 1:1 with 50 mM potassium phosphate buffer (pH 8) and ultracentrifuged at 255000*g* at 4 °C for 60 min. The resulting supernatant was applied on a linear sucrose gradient (3 to 17% w/v), containing 1% Deriphat-160 and 0.5% *n*-octyl-β-D-glucoside, and centrifuged at 80000*g* for 12 h at 4 °C. The band corresponding to the LHI−RC complexes was collected, diluted three times with 25 mM Tris-HCl, pH 7.8, containing 1% Deriphat-160 and concentrated by ultrafiltration on a PM 100000 membrane (Millipore). The absorption spectrum presents a major absorption band at 887 nm characteristic of the LHI core antenna complexes.

Purification of the Soluble Carriers and Preparation of Membranes. The periplasmic carriers and membrane fragments were purified as described elsewhere (Schoepp et al., 1995). The crude periplasmic fraction was applied to a CM-23 column equilibrated with 20 mM Tris-HCl (pH 6) at 4 °C. Using a linear salt gradient (0−100 mM NaCl), HiPIP, cyt *c*′, cyt c_8, and a low redox potential c_{550} were eluted from the column. The fractions containing HiPIP or cyt c_8 were concentrated, dialyzed against 20 mM Tris-HCl (pH 6), and purified by gel filtration on Sephadex G-100. Estimation of the amount of cyt c_8 in the crude periplasmic fraction was made using the extinction coefficient of 19 mM^{-1} cm^{-1} at 551 nm, on a (native − oxidized) difference absorption spectrum. HiPIP concentration was determined by EPR spectroscopy using a standard solution.

Redox Titrations of the Tetrahemic Cytochrome and Light-Induced Absorption Changes. Redox titration of the tetraheme cytochrome was achieved by measurements of light-induced absorption changes in purified membranes suspended in 25 mM Tris-HCl (pH 7.8). In addition, dark titration was performed on LHI−RC complexes suspended in 25 mM Tris-HCl, pH 8, and 1% Deriphat-160. Equilibration with the electrode was achieved by adding the following mediators, each at 10 μM concentration: diaminodurene (E_m = +260 mV), 1,2-naphtoquinone-4-sulfonic acid (+215 mV), 1,2-naphtoquinone (+145 mV), phenazine methosulfate (+80 mV), duroquinone (+5 mV), and 2-OH-1,4-naphtoquinone (−140 mV). Redox potentials were adjusted by addition of small aliquots of 10 mM potassium ferricyanide, 10 mM sodium ascorbate, and 10 mM sodium dithionite. Redox potentials were measured with a combined Ag/AgCl reference system electrode (INGOLD) and are given relative to the normal hydrogen electrode. Curve fitting was carried out with a nonlinear regression data analysis program (1987, BIOSOFT, Enzfitter 1.05). The photo-induced absorbance changes were recorded with a home-built flash kinetics spectrophotometer (Joliot et al., 1980). The actinic light was provided by a xenon lamp (flash duration 3 μs) or by an Alexandrite laser (780 nm, 100 ns flash duration, 50 mJ, Laser 1-2-3, Schwartz Electro Optics). Absorption spectra at 77 K were performed on an AMINCO DW2a spectrophotometer equiped with a low-temperature accessory.

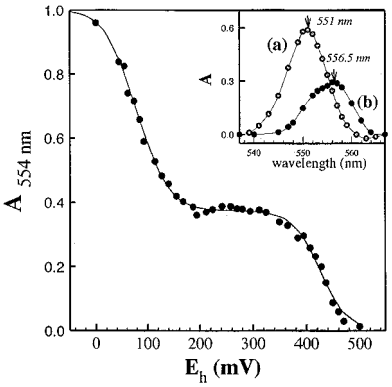

FIGURE 1: E_h dependence of the absorption measured in the α-band for LHI−RC complexes suspended in 25 mM Tris-HCl, pH 8, 1% Deriphat-160. Absorption measurements were performed at 554 nm, a wavelength located between the λ_{max} of the LP hemes (551 nm) and those of the HP (557 nm) hemes. The solid line was obtained with the theoretical redox titration curve using the following values for the redox parameters: $E_m(HP_1) = E_m(HP_2) = 420$ mV, $E_m(LP_1) = 110$ mV, $E_m(LP_2) = 60$ mV. The dotted line was obtained when assuming a sum of four $n = 1$ Nernst curves with the same redox parameters. (Inset) Difference absorption spectra recorded in the α-band at different redox potentials: (a) +45 mV − +240 mV (LP hemes), (b) +385 mV − +470 mV (HP hemes).

Linear Dichroism Spectra. LD spectra were recorded in RC−LHI complexes into squeezed polyacrylamide gel as described before (Haworth et al., 1982; Tapie et al., 1982). The different redox states were obtained by incubation overnight in 27 mM Tris-HCl, 60% glycerol with 100 mM ferricyanide, 100 mM DAD/10 mM ascorbate, or 100 mM sodium dithionite. The LD spectra were recorded at low temperature (10 K) on a home-built spectrophotometer as described previously (Breton, 1974; Tapie et al., 1982). To compute the orientation, we used the function $LD/A = 3/2\alpha(3\cos^2\beta - 1)$ where LD is the linear dichroism, A the absorption signal, α the statistical orientation factor of the sample in the polyacrylamide gel, and β the angle between the transition and the orientation axis. For a heme with two energetically distinct transitions Q_x and Q_y, the angle N between the normal of the plane and the orientation axis can be calculated with: $\sin^2 N = \cos^2\beta_x + \cos^2\beta_y$, where β_x and β_y correspond to angles between the Q_x and Q_y transitions, respectively, and the orientation axis. When transitions are energetically equivalent, only the orientation N of the normal is calculated by $LD/A = 3/4\alpha(1 - \cos^2 N)$. The LD and absorption spectra were deconvoluted into the individual optical transitions by using the Sigma Plot software (Jandel Scientific).

RESULTS

Oxido-Reduction and Spectral Properties of the RC Bound Cytochrome. Figure 1 shows a typical redox titration curve (between 500 and 0 mV) of the RC bound cytochrome monitored at 554 nm in particles of LHI−RC complexes at pH 7.8. The high-potential wave, between 500 and 300 mV, corresponds to the reduction of the two HP hemes while the second wave between 200 and 0 mV corresponds to the LP hemes reduction. The smaller amplitude of the high-potential wave compared to the low-potential one is due to the difference in ϵ [(millimolar)$^{-1}$ (centimeters)$^{-1}$] in between the HP and the LP hemes at 554 nm (see inser). In order to fit the redox titration of the four hemes, we made the assumption of a negligible interaction between the individual hemes (i.e., the redox state of one does not affect the E_m of another). The solid line in Figure 1 gives the best fit with a sum of four $n = 1$ Nernst curves. The E_ms of the two HP hemes thus obtained are identical (+420 mV), i.e., they titrate following a single Nernst curve. For the E_ms of the LP hemes, we obtained different E_m values of +110 and +60 mV. The large difference in the mid-point potentials of the HP and LP hemes allows us to determine the positions of their α-bands (Figure 1, inset). The α-band of the HP hemes peaks at 556−557 nm with a shoulder at 553 nm (Figure 1, curve b), as shown by the difference between spectra recorded at +385 and +470 mV. The difference between the spectra recorded at +45 and +240 mV shows an α-band centered at 551 nm for the LP hemes (Figure 1, curve a).

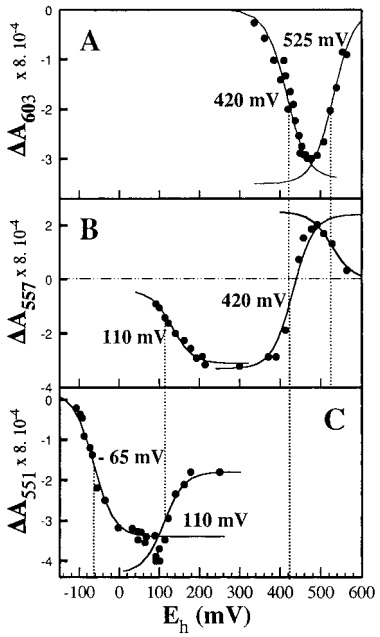

FIGURE 2: E_h dependence of the light-induced absorption recorded at 50 μs after the actinic flash, on membranes of *Rc. tenuis* ([RC] = 120 nM) suspended in 25 mM Tris-HCl (pH 7.8) at (A) 603 nm (RC), (B) 557 nm (HP hemes), and (C) 551 nm (LP hemes). Experimental values were fitted with n = 1 Nernst equations (solid lines).

The light-induced absorption changes linked to the photo-oxidation of the primary electron donor P of the HP hemes and the LP hemes were detected 50 μs after the exciting flash at 603, 557, and 551 nm, respectively, as a function of the ambient redox potential (E_h) in purified membranes of *Rc. tenuis* (Figure 2). As the ambient potential was lowered from 580 to 480 mV, there was an increase in the amount of primary donor remaining oxidized 50 μs after an actinic flash, but below about 480 mV, it decreased again (Figure 2A). This behavior can be fitted with two $n = 1$ Nernst curves. The first Nernst curve corresponds to the E_m of P^+/P, found to be equal to +525 ± 10 mV. The disappearance of the P^+ signal for E_h values lower than 480 mV is due to its rapid rereduction by the HP hemes, corresponding to a Nernst curve at $E_m = +420$ mV (± 10 mV). At 557 nm, the light-induced absorption changes are positive at high E_h, due to the spectral contribution of P^+ (Figure 2B). The signal becomes negative when lowering the E_h, due to the photo-oxidation of the HP hemes. The E_m obtained with the $n = 1$ Nernst fit curve (+420 mV) is in agreement with the mid-point potentials of these hemes (Figure 1). Below 200 mV, the photo-oxidation of the HP hemes decreases, because the

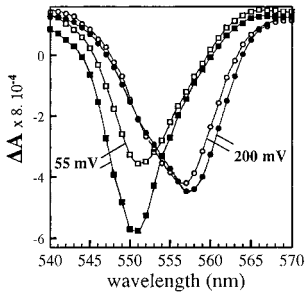

FIGURE 3: Light-induced absorption spectra in the α-band recorded on membranes of *Rc. Tenuis* ([RC] = 230 nM) suspended in 25 mM Tris-HCl (pH 7.8). Redox potentials were poised at 200 mV (○ and ●) and 55 mV (□ and ■). For each redox potential, the signal was measured after a first laser flash (● and ■) and a second xenon flash (○ and □) separated by 10 ms.

photo-oxidized primary donor becomes now rereduced by the LP hemes. This is clearly shown by the light-induced absorption changes recorded at 551 nm. At this wavelength (Figure 2C), the amplitude of the light-induced signal is constant between 300 and 200 mV. This corresponds to the contribution of photo-oxidized HP hemes at 551 nm. At ambient potentials lower than 200 mV, the amplitude of light-induced signal increases. This increase can be fitted with a $n = 1$ Nernst curve corresponding to the E_m value of the LP_1 heme, +110 mV. Below 0 mV, the amplitude decreases because of the reduction of the primary acceptor. The fitting curve gives a mid-point potential for the redox couple Q_A/Q_A^- equal to −65 mV (± 10 mV) at pH 7.8. This value is higher than those measured at pH 7.8 in *Rp. viridis* (E_m = −140 mV; Cogdell & Crofts, 1972; Prince et al., 1976) and in *C. vinosum* (E_m = −150 mV, Prince & Dutton, 1976; Jackson et al., 1973), but is similar to the one obtained for *Rb. sphaeroides* (E_m = −70 mV; Dutton et al., 1973; Jackson et al., 1973). Note that between 100 and 60 mV the amplitude of the signal at 551 nm slightly increases. This might be due to the photo-oxidation of LP_1 heme in this redox range possessing a slightly higher ϵ [(millimolar)$^{-1}$ (centimeters)$^{-1}$] than the LP_2 heme. To determine the absorption peak of each of the four hemes in the α-band, light-induced absorption spectra have been recorded in membranes maintained at two redox potentials (200 and 55 mV), with a train of two actinic flashes (Figure 3). The first flash and the second flash are spaced by 10 ms, to prevent rereduction of the tetraheme cyt between flashes. At 200 mV, the two HP hemes are reduced and can be photo-oxidized. No significant difference in the α-band position of the hemes photo-oxidized upon each flash is visible: in both cases, the α-band peaks at 557 nm and presents a shoulder at 553 nm in agreement with the results of Figure 1. These similar spectra can be due to the close mid-point potential values of the two HP hemes: the first flash oxidizes almost equivalent amounts of HP_1 and HP_2, as does also the second flash. At E_h = 55 mV, the first flash oxidizes mostly the LP_1 heme and the second flash the LP_2 heme. The α-bands of LP_1 and LP_2 are slightly distinct and centered at 550.5 and 551 nm, respectively.

Absorption and Linear Dichroism Spectra at Low Temperature. Absorption spectra in the α-band region of LHI−RC complexes have been recorded at low temperature (77 K) for different redox conditions (Figure 4). The absorption spectra of the high-potential hemes can be obtained by recording a DAD − ferricyanide difference spectrum (Figure

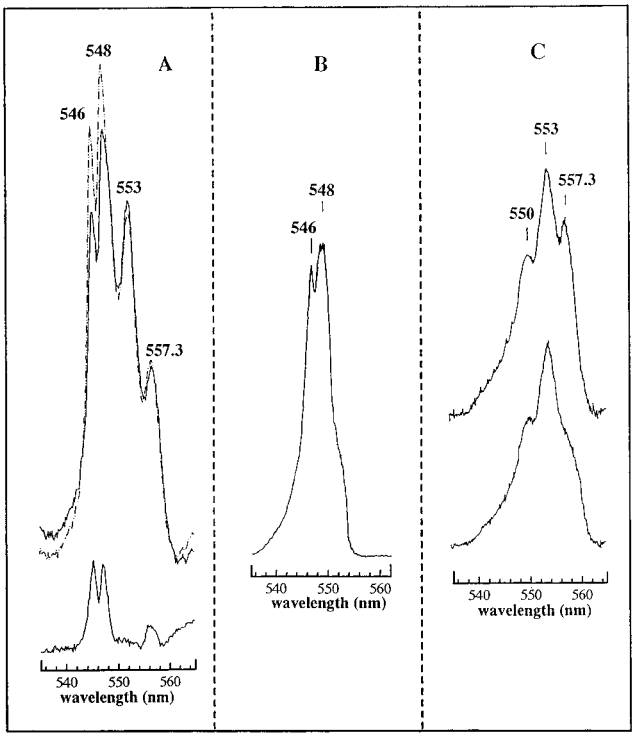

FIGURE 4: Absorption spectra recorded at 77 K for a suspension of LHI−RC complexes isolated from *Rc. tenuis* in different redox conditions: (A) at +25 mV (solid line) and −50 mV (dashed dotted line). The lower spectrum represents the difference spectrum between these two redox conditions. (B) Dithionite 1 mM − DAD 1 mM difference spectrum. (C) DAD 1 mM − ferricyanide 20 mM (upper spectrum) and ferricyanide 100 μM − 20 mM (lower spectrum).

4C). This difference spectrum presents three peaks at 553, 550, and 557 nm. If the high-potential hemes are only partially oxidized by addition of 100 μM potassium ferricyanide, the 557 nm peak appears only as a shoulder. This indicates that the absorption contribution of the two high-potential hemes can be distinguished at low temperature. From this series of experiments, we deduce that the 550 and 553 nm transitions belong to the heme which possesses the highest mid-point potential (HP_1). The second high-potential heme (HP_2) absorbs at 553 and 557 nm. The dithionite − DAD difference spectrum (Figure 4B) corresponds to the absorption of the low-potential hemes. This spectrum presents two distinct transitions peaking at 546 and 548 nm. We attempted to determine the spectral contribution of each of the two low-potential hemes by calculating the difference spectrum between two redox potentials of −50 and +25 mV (Figure 4A, lower spectrum). Since both of the signals corresponding to the transitions centered at 546 and 548 nm decrease when increasing the redox potential, this implies that the lowest mid-point potential heme (LP_2) absorbs at these two wavelengths. The spectral contribution of the LP_1 is difficult to determine from the above experiments. This heme can present either two transitions at 546 and 548 nm or a single transition around 548 nm.

Linear dichroism and absorption spectra of LHI−RC complexes of *Rc. tenuis* oriented in squeezed poyacrylamide gels have been recorded at 10 K under reducing or oxidizing conditions in the 540−565 nm region (Figure 5). Under oxidizing conditions, the only transition observed in this spectral region absorbs at 545 nm (Figure 5, curve b of panels A and B). This corresponds to the Q_x transition of the Bpheo

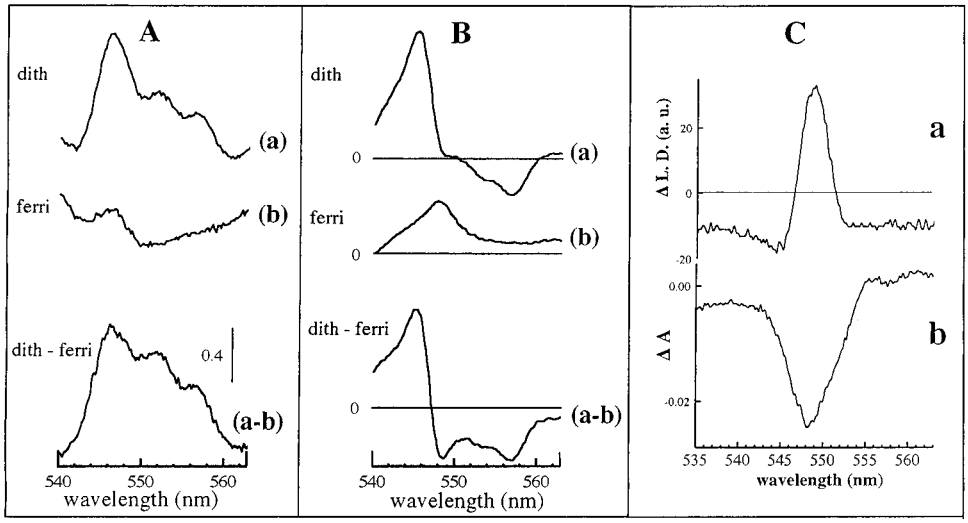

FIGURE 5: Absorption spectra (A) and linear dichroism (B) recorded at 10 K for LHI−RC complexes reduced with sodium dithionite 100 mM (curve a), or oxidized with ferricyanide (curve b). The lower spectrum represents the difference between a and b spectra. (C) Light-induced difference linear dichroism (a) and absorption spectra (b) obtained by a continuous illumination at 10 K on LHI−RC complexes reduced by addition of 100 mM ascorbate. Note that the two transitions centered at 546 and 548 nm are not resolved in the absorption spectra, compared to Figure 4, because of the larger band width of the monochromator used in this experiment.

molecule localized along the L-branch. This transition gives a positive signal in the LD spectrum. To obtain the contribution of the four hemes in the LD spectrum, the RC bound cytochrome was reduced by addition of sodium dithionite (Figure 5, curve a of panels A−C). The LD contribution of the four hemes consists of three negative bands centered at 557, 553, and 549 nm and a positive band centered at 546 nm. This appears in the LD difference spectrum between reduced and oxidized samples (Figure 5B, bottom spectrum) which eliminates the contribution of the Bpheo Q_x. According to the spectral attribution for the HP hemes we have made above, their corresponding LD spectrum can be interpreted as follows. The two transitions of the HP_2 heme (553 and 557 nm) present null and negative values, respectively. The LD values for the two transitions of HP_1 (550 and 553 nm) are close to 0. To take into account the unknown degree of orientation of the LHI−RC particules in the gel, we normalized the LD/A values by assuming that the 545 nm Q_x transition of the Bpheo of *Rc. tenuis* makes an angle of 81° with the C2 axis of the RC, i.e., a value similar to that determined for *Rp. viridis* RCs (Deisenhofer et al., 1985). This assumption is justified by the very similar respective orientation of RC chromophores determined so far for different species of photosynthetic bacteria. We can then calculate the angle between the normal of the HP_1 and HP_2 heme planes and the C2 symetry axis of the RCs as equal to 55 ± 5° and 67 ± 5°, respectively. The overlap of the transitions of the two LP hemes renders difficult the discrimination of their respective contribution in the 546−550 nm region. Figure 5C shows the LD and absorption difference spectra induced by continuous illumination at 10 K in a sample reduced by addition of 100 mM ascorbate. The light-induced absorption difference spectrum is centered at 549 nm, indicating that only the LP_1 heme has been photo-oxidized in these conditions. If some photo-oxidation of the LP_2 heme would have occurred, one would have observed the bleaching of its two transitions centered at 546 and 548 nm (Figure 4A). LD and absorption difference spectra are slightly different in shape, the bleached band observed in the light-induced difference LD spectrum (Figure 5C, curve a) being narrower than the one of the light-induced difference absorption spectrum (Figure 5C, curve b). One way to interpret these results is to suppose that the LP_1 heme possesses two distinct transitions absorbing around 549 nm and that the transition of lower energy (long wavelength side) possesses a negative LD/*A* value of about −1.1, while the LD/*A* value of the higher energy transition (short wavelength side) is slightly positive. One can then deduce that the angle between the normal of the heme and the C2 axis is equal to 73 ± 5°. Knowing the LD/*A* value and the position wavelength of LP_1, the LD/*A* values for the transitions of the LP_2 heme are deduced by fitting the LD and absorption spectra, in the 540−550 nm region for a totally reduced sample of LHI−RC particles (Figure 5B). This leads to an angle of 45 ± 5° between the normal of the LP_2 heme and the C2 axis.

HP Hemes Reduction by HiPIP and Cyt c_8. Because of the high value of E_m of the HP hemes, both HiPIP (E_m = +304 mV) and cyt c_8 (E_m = +405 mV) can play a significant role in the photosynthetic electron transport. To verify this hypothesis, reconstitution experiments were made with membranes of *Rc. tenuis* and these two electron carriers. Purified membranes of *Rc. tenuis* were poised at about 260 mV, a redox potential at which the HP hemes are fully reduced, and light-induced absorption changes were recorded in the absence and presence of soluble electron donors. In the absence of any added soluble electron carrier, the HP hemes reduction, measured at 561−540 nm, is very slow ($t_{1/2}$ > 1 s) (Figure 6, curve a of panels A, C, and D). Upon addition of 1.1 μM cyt c_8 to membranes (RC = 560 nM), a large part of the photo-oxidized HP hemes is rapidly rereduced. The half-time of this fast phase is about 20 ms (Figure 6A, curve b). Kinetics of absorption changes recorded at 547 nm, linked to the cyt c_8 oxidation, reveal also a half-time of 20 ms. Light-induced absorption spectra in the α-band were monitored at 1 and 20 ms after the actinic flash in the presence of cyt c_8 (Figure 6B). A wavelength shift from 557 to 554 nm occurs in the 1−20 ms time range. This is clearly shown in the difference spectrum (dotted line) which presents an oxidation peak at 551 nm. These results are consistent with electron transfer from the cyt c_8 to the HP hemes with a half-time of 20 ms.

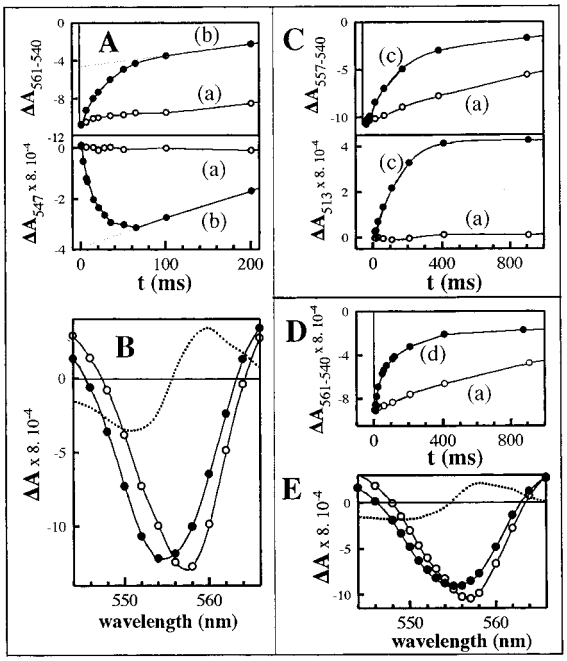

FIGURE 6: Kinetics of light-induced absorbance changes recorded in purified membrane fragments of *Rc. tenuis* suspended in 20 mM Tris-HCl (pH 7.5), supplemented or not by HiPIP, cyt c_8, or the crude periplasmic fraction. The redox potential was poised at 260 mV by addition of 20 μM DAD and 20 μM sodium ascorbate. Kinetics of the HP hemes rereduction was measured at the maximum of the α-band (557−540 nm) or at (561−540 nm) when cyt c_8 was added to minimize its contribution in the absorption changes. Absorption changes related to the HiPIP oxidation were measured at 513 nm. (A) On membrane fragments ([RC] = 560 nM) without addition (curve a) or supplemented with 1.1 μM cyt c_8 (curve b), (C) on membranes fragments ([RC] = 400 nM) without (a) or with 1 μM HiPIP (curve c), and (D) on membranes ([RC] = 500 nM) with the periplasmic fraction (1.2 μM HiPIP and 0.5 μM cyt c_8) (curve d). Light-induced difference spectra in the α-band, recorded at 1 ms (▽) and 20 ms (▼) after the flash excitation, were plotted for membrane fragments supplemented with panel B, 1.1 μM cyt c_8, and panel E, the periplasmic fraction. The dotted lines correspond to the difference between the spectum recorded 20 ms and 1 ms after the actinic flash.

Upon addition of 1 μM HiPIP to membranes (RC = 400 nM) poised at 260 mV, the HP heme rereduction occurs with a $t_{1/2}$ of about 140 ms, as shown by the absorption changes recorded at 557−540 nm (Figure 6C, curve c). As the extinction coefficient of the oxidized HiPIP is maximal between 480 and 520 nm (broad peak), kinetics of HiPIP oxidation was recorded at 513 nm, an isosbestic point for the carotenoid band-shift, where the cyt contribution is small. The light-induced absorption changes observed at 513 nm are positive in agreement with the occurrence of an HiPIP oxidation. The kinetics of HiPIP oxidation gives a similar half-time value as in the heme absorption region. The amplitude of the absorption changes at 513 nm corresponds to 425 nM of photo-oxidized HiPIP using an extinction coefficient of 8 mM^{-1} cm^{-1}, in reasonable agreement with the concentration of the RC. This demonstrates that HiPIP can act as an efficient electron donor to the RC bound tetraheme.

Addition of the crude periplasmic fraction, containing about 1.2 μM HiPIP and 0.5 μM cyt c_8 to membranes (RC = 500 nM) poised at 260 mV, induces a fast HP heme reduction measured at 561−540 nm ($t_{1/2}$ = 100 ms) (Figure 6D, curve d). Figure 6E shows the light-induced absorption spectra in the α-band monitored 1 and 20 ms after the actinic flash, upon addition of the periplasmic fraction. The absorption changes associated with the cyt c_8 oxidation are small compared with those of Figure 6B.

DISCUSSION

In the RC bound cyt, the four redox sites are closely packed and may interact with each other. The interaction potentials between the four sites have been estimated for the tetraheme cyt c_3 from *Desulfovibrio desulfuricans* (Gayda et al., 1988) and *Desulfovibrio vulgaris* (Benosman et al., 1989). These authors have demonstrated that the conformation of the heme with the lowest redox potential, heme 4, is sensitive to the redox state of the heme with the highest potential, heme 1. Our redox titration data (Figure 1) is satisfactorily fitted using a sum of four $n = 1$ Nernst curves thus neglecting possible interactions. This gives, within experimental accuracy, a single E_m value for both HP hemes (+420 mV) and E_ms of +110 mV (LP_1) and +60 mV (LP_2) for the LP hemes. This good fit given thus obtained does not ascertain, however, the absence of interactions. On the first hand, the large difference (>300 mV) between the two groups of hemes precludes any statement on the interaction between them. Indeed, the LP hemes titrate out when the HP hemes are fully reduced, so that a possible interaction would only shift the apparent positions of the E_ms, without distorting the curves otherwise. On the other hand, interaction between the two HP hemes or between the two LP hemes cannot be ruled out on the sole basis of their apparent Nernstian behavior. The good simulations obtained do show, however, that such interaction potentials should be relatively small, especially in the case of the HP hemes. This question could be addressed by titrating individually each heme. This cannot be done by absorption measurements (because the individual spectra are too close) but may be feasible by EPR. Indeed, several works (Nitschke & Rutherford, 1989; Nitschke et al., 1992, 1993) have shown that the spectral contribution of each heme can be clearly distinguished by the g_z peak in the EPR spectrum, allowing the determination of their microscopic mid-point potential. A similar detailed EPR study is necessary in the case of *Rc. tenuis* to determine the redox characteristic of each individual heme and the interaction energies between them.

Keeping in mind this restriction, we may compare the mid-point potentials we determined in the case of the tetraheme cyt of *Rc. tenuis* with those measured in different photosynthetic species. The mid-point potential values of the LP hemes of proteobacteria fall into two classes [see Nitschke and Dracheva (1995)]. For some species, these values are low and comprised between +50 and −80 mV. On the other hand, higher values, in the range +90−130 mV, have been measured in the case of *Ru. gelatinosus* (+130, +70 mV) (Fukushima et al., 1988; Nitschke et al., 1992), *Rp. acidophila* (+110, +110 mV) (Matsuura & Shimada, 1986), and *R. denitrificans* (+90, +90 mV) (Garcia et al., 1994). The characteristics we have determined for the tetraheme cyt of *Rc. tenuis* (+110, +60 mV) fall into this second group. The E_m of the HP hemes (+420 ± 10 mV) in *Rc. tenuis* are significantly higher than those already determined for other purple bacteria: +320 and +300 mV for *Ru. gelatinosus* (Fukushima et al., 1988; Nitschke et al., 1992), +360 and +312 mV for *Rp. viridis* (Dracheva et al., 1986), +354 and +294 mV for *Rf. fermentans* (Hochkoeppler et al., 1995). However, because the mid-point potential of the primary

Table 1. Orientation of the Hemes of RC Bound Cytochromes with Respect to the Membrane Plane for Different Bacteria Species

	Rc. tenuis (this work)	*Ru. gelatinosus*[a]	*C. vinosum*[b]	*Rp. viridis*[c]	*R. denitrificans*[d]	*C. aurantiacus*[e]
HP_1	55 ± 5°	0°	30°	80°	40°	30°
HP_2	67 ± 5°	90°	90°	55°	55°	90°
LP_1	73 ± 5°	90°	0 or 40°	60°	90 or 40°	40−50°
LP_2	45 ± 5°	0°	40 or 0°	85°	40 or 90°	45°

[a] Nitschke et al. (1992). [b] Nitschke et al. (1993). [c] Verméglio et al. (1989a). [d] Garcia et al. (1994). [e] Van Vliet et al. (1991).

electron donor of *Rc. tenuis* is also rather high (+525 mV), the ΔE between this E_m and the one of HP_1 is equal to 100 mV, a value very similar to the one measured for the majority of species possessing a RC bound tetraheme cyt. In *Rc. tenuis*, we therefore expect the same order of magnitude for the rate of electron transfer between HP and P than those determined for the species studied so far. Moreover, the difference between the mid-point potentials of the primary donor and the primary acceptor ($\Delta E_m = +590$ mV at pH 7.8 in *Rc. tenuis*) is higher than the one measured in *Rb. sphaeroides* at the same pH ($\Delta E_m = +520$ mV), but is smaller than those obtained in *C. vinosum* and *Rp. viridis* ($\Delta E_m = +640$ and +630 mV, respectively).

Because of the high E_m values of HP_1 and HP_2, the two high-potential soluble carriers present in the periplasm of *Rc. tenuis*, HiPIP ($E_m = +304$ mV) and cyt c_8 ($E_m = +405$ mV), are putative electron donor to the RC bound tetraheme cyt. Reconstitution experiments demonstrate that, indeed, both HiPIP and cyt c_8 are efficient electron donors to the HP hemes of the RC bound tetraheme cyt. Despite the fact that the HiPIP has a much more favorable redox potential than cyt c_8 to be an efficient electron donor to the HP heme(s), the faster rate measured is between the cyt c_8 and the RC bound tetraheme ($t_{1/2} \approx 20$ ms). This lack of correlation between driving force and rate contants emphasizes that other factors, such as distance, relative orientation of redox centers, and different binding affinities of HiPIP and cyt c_8 for the tetraheme, influence the mechanism of interproteins electron transfer. A complete study of the HiPIP and cyt c_8 concentration and ionic strength dependence on the electron transfer kinetics is in progress to address the different implicated parameters. Upon addition of the crude periplasmic fraction, the half-time of HP heme reduction is in the same order of magnitude as that measured upon addition of the isolated HiPIP (about 100 ms). Moreover, the light-induced absorption spectrum in the α-band shows only a small participation of the cyt c_8 in the electron transfer. These observations suggest that upon addition of the total soluble fraction, the HiPIP is the main soluble electron donor. This result can be explained by the excess of reduced HiPIP in the periplasmic space compared to reduced cyt c_8 at the E_h of the experiment. From EPR and absorption analysis, we determined this ratio to be 2.5 (data not shown). At 260 mV, 85% of the HiPIP is reduced so that the ratio $[HiPIP]_{red}/[cyt\ c_8]_{red}$ is about 2. An additional explanation could be a competitive inhibition of the cyt c_8 binding by the HiPIP, possibility related to the difference in net charge between HiPIP (+5) and cyt c_8 (+4).

The hemes orientations determined so far for different species of photosynthetic bacteria [see Nitschke and Dracheva (1995) for a review) appear to be rather different from one another (Table 1). The tetraheme of *Rc. tenuis* presents no clear similarity with other determined arrangements (Table 1). This nonconservation of heme orientations between species is related to the low sequence homology in the tetraheme polypeptide regions in contact with the core RC. The different orientation of hemes with respect to the membrane plane may reflect the capability of the tetraheme to react with soluble electron carriers of different nature. In this context, it is worth remembering that, in the case of *Rp. viridis*, the best electron donor to the tetraheme is cyt c_2. The cyt c_8 of *Rc. tenuis* or HiPIPs isolated from *Ru. gelatinosus*, *Rp. marina*, or *Rhodospirillum salinarum* react only very slowly with the *Rp. viridis* reaction center (Meyer et al., 1993). On the other hand, both HiPIP and cyt c_8 can rereduce efficiently the RC bound tetraheme cyt of *Ru. gelatinosus* (Schoepp, 1994; Schoepp et al., 1995) and of *Rc. tenuis* (this work).

In conclusion, the tetraheme subunit of RC of *Rc. tenuis* appears to present several similitudes with other described tetraheme cyt. As for all the species studied so far, with the exception of *Rhodospirillum molischianum* (Nagashima et al., 1993), this tetraheme subunit possesses one pair of HP hemes and one pair of LP hemes. The relative orientations of the four hemes of *Rc. tenuis* correspond, however, to none of those described so far. This is however not surprising since, with the exception of the closely related species *Rp. viridis* and *Rp. sulfoviridis* (Verméglio et al., 1989a), all the tetraheme cyt present a different heme arrangement. The main particularity of the *Rc. tenuis* tetraheme is the value of the mid-point potentials of the HP hemes (+420 mV), the highest reported so far. This is correlated with their *in vivo* rereduction by the cyt c_8 as described in the following article in this issue.

ACKNOWLEDGMENT

The authors whish to thank Dr. J. Breton for allowing the use of his home-built LD spectrophotometer, Dr. J. Gaillard for recording EPR spectra, and Dr. J. Lavergne for usefull discussions. The technical assistance of A. LeMouellic has been greatly appreciated.

REFERENCES

Agalidis, I., Ivancich, A., Mattioli, T. A., & Reiss-Husson, F. (1997) *Biochim. Biophys. Acta 1321*, 31−46.
Alegria, G., & Dutton, P. L. (1990) *Biophys. J. 57*, W-Pos607.
Alegria, G., & Dutton, P. L. (1991) *Biochim. Biophys. Acta 1057*, 258−272.
Allen, J. P., Feher, G., Yeates, T. O., Rees, D. C., Deisenhofer, J., Michel, H., & Huber, R. (1986) *Proc. Natl. Acad. Sci. U.S.A. 83*, 8589−8593.
Benosman, H., Asso, M., Bertrand, P., Yagi, T., & Gayda, J. P. (1989) *Eur. J. Biochem. 182*, 51−55.
Breton, J. (1974) Thesis, Paris, France.
Bruce, B. D., Fuller, R. C., & Blankenship, R. E. (1982) *Proc. Natl. Acad. Sci. U.S.A. 79*, 6532−6536.
Case, G. D., & Parson, W. W. (1971) *Biochim. Biophys. Acta 253*, 187−202.
Case, G. D., & Parson, W. W. (1973) *Biochim. Biophys. Acta 325*, 441−453.

Clayton, R. K., & Clayton, B. J. (1978) *Biochim. Biophys. Acta 501*, 478−487.
Cogdell, R. J., Jackson, J. B., & Crofts, A. R. (1972) *Bioenergetics* 4, 211−227.
Davies, B. H., & Than A. (1974) *Phytochemistry 13*, 209−219.
Deisenhofer, J., Epp, O., Miki, K., Huber, R., & Michel, H. (1985) *Nature 318*, 618−624.
Dracheva, S. M., Drachev, L. A., Zaberezhnaya, S. M., Konstantinov, A. A., Semenov, A.Y., & Skulachev, V. P. (1986) *FEBS Lett. 205*, 41−46.
Dracheva, S. M., Drachev, L. A., Konstantinov, A. A., Semenov, A. Y., Skulachev, V. P., Arutjunjan, A. M., Shuvalov., V. A., & Zaberezhnaya, S. M. (1988) *Eur. J. Biochem. 171*, 253−264.
Dutton, P. L. (1971) *Biochim. Biophys. Acta 226*, 63−80.
Dutton, P. L., & Prince, R. C. (1978) in *The Photosynthetic Bacteria* (Clayton, R. K., & Sistrom, W. R., Eds.) pp 525−570, Plenum Press, New York.
Dutton, P. L., Leigh, J. S., & Wraight, C. A. (1973) *FEBS Lett. 36*, 169−173.
Freeman, J. C., & Blankenship, R. E. (1990) *Photosynth. Res. 23*, 29−38.
Fritzsch, G., Buchanan, S., & Michel, H. (1989) *Biochim. Biophys. Acta 977*, 157−162.
Fukushima, A., Matsuura, K., Shimada, K., & Satoh, T. (1988) *Biochim. Biophys. Acta 933*, 399−405.
Garcia, D., Richaud, P., & Verméglio, A. (1994) *Biochim. Biophys. Acta 1144*, 295−301.
Gayda, J. P., Benosman, H., Bertrand, P., More, C., & Asso, M. (1988) *Eur. J. Biochem. 177*, 199−206.
Haworth, P., Tapie, P., Arntzen, C., & Breton, J. (1982) *Biochim. Biophys. Acta 682*, 152−159.
Hochkoeppler, A., Venturoli, G., & Zannoni, D. (1993) *Biol. Chem. Hoppe-Seyler 374*, 831.
Hochkoppler, A., Moschettini, G., & Zannoni, D. (1995) *Biochim. Biophys. Acta, 1229*, 73−80.
Hu, Q., Brunisholz, R. A., Franck, G., & Zuber H. (1996) *Eur. J. Biochem. 238*, 381−390.
Jackson, J. B., Cogdell, R. J., & Crofts, A. R. (1973) *Biochim. Biophys. Acta 290*, 218−225.
Joliot, P., Béal, D., & Frilley, B. (1980) *J. Chim. Phys. 77*, 209−216.
Malhotra, H. G., Britton, G., & Goodwin, T. W. (1969) *Phytochemistry 8*, 1047−1049.
Matsuura, K., & Shimada, K. (1986) *Biochim. Biophys. Acta 852*, 9−18.
Matsuura, K., Fukushima, A., Shimada, K., & Satoh, T. (1988) *FEBS Lett. 237*, 21−25.
Meyer, T. E., & Donohue, T. J. (1995) in *Anoxygenic Photosynthetic Bacteria* (Blankenship, R. E., Madigan, M. T., & Bauer, C. E., Eds.) pp 725−745, Kluwer Academic Publishers, Dordrecht.
Meyer, T. E., Bartsch, R. G., Cusanovich, M. A., & Tollin T. (1993) *Biochemistry 32*, 4719−4726.
Nagashima, K. V. P., Itoh, S., Shimada, K., & Matsuura, K. (1993) *Biochim. Biophys. Acta 1140*, 297−303.
Nitschke, W., & Rutherford, A. W. (1989) *Biochemistry 28*, 3161−3168.
Nitschkle, W., & Dracheva, S. M. (1995) in *Anoxygenic Photosynthetic Bacteria* (Blankenship, R. E., Madigan, M. T., & Bauer, C. E., Eds.) pp 775−805, Kluwer Academic Publishers, Dordrecht.
Nitschke, W., Agalidis, I., & Rutherford, A. W. (1992) *Biochim. Biophys. Acta 1100*, 49−57.
Nitschke, W., Jubault-Bregler, M., & Rutherford, A. W. (1993) *Biochemistry 32*, 8871−8879.
Prince, R. C., & Dutton, P. L. (1976) *Arch. Biochem. Biophys. 172*, 329−334.
Prince, R. C., & Olson, J. M. (1976) *Biochim. Biophys. Acta 423*, 357−362.
Prince, R. C., Leigh, J. S., & Dutton, P. L. (1976) *Biochim. Biophys. Acta 440*, 622−636.
Prince, R. C., Dutton, P. L., Clayton, B. J., & Clayton, R. K. (1978) *Biochim. Biophys. Acta 502*, 354−358.
Prince, R. C., Gest, H., & Blankenship, R. E. (1985) *Biochim. Biophys. Acta 810*, 377−384.
Schoepp, B., (1994) Thesis, Paris-Grignon, France.
Schoepp, B., Parot, P., Menin, L., Gaillard, J., Richaud, P., & Verméglio, A. (1995) *Biochemistry 34*, 11736−11742.
Tapie, P., Haworth, P., Hervo, G., & Breton, J. (1982) *Biochim. Biophys. Acta 682*, 339−344.
Van Vliet, P., Zannoni, D., Nitschke, W., & Rutherford, A. W. (1991) *Eur. J. Biochem. 199*, 317−323.
Verméglio A., Garcia, D., & Breton, J. (1989a) in *Reaction Centers of Photosynthetic Bacteria* (Michel-Beyerle, M. E., Ed.) Springer Series in Biophysics, Vol. 6, pp 19−22, Springer-Verlag, Berlin.
Verméglio, A., Richaud., P., & Breton, J. (1989b) *FEBS Lett. 243*, 259−263.
Zannoni, D., & Venturoli, G. (1988) in *Green Photosynthetic Bacteria* (Olson, J. M., Ormerod, J. G., Amesz, J., Stackebrandt, E., & Trüper, H. G., Eds.) pp 135−143, Plenum Press, New York.

BI971162J